

BY WILLIAM M. BALCH AND PAUL E. UTGOFF

POTENTIAL INTERACTIONS AMONG OCEAN ACIDIFICATION, COCCOLITHOPHORES, AND THE OPTICAL PROPERTIES OF SEAWATER

Suspended calcium carbonate in the sea plays a major role in the ocean's optical properties due to its strong light scattering. To illustrate this phenomenon, four views of a black optical sensor are shown as it is lowered into a bloom of coccolithophores—algae that cover themselves with 0.2- μm -diameter calcium carbonate plates called coccoliths (sampled just north of the Malvinas/Falklands Islands, December 2008). From top to bottom: sensor just under the sea surface; sensor at ~ 0.5 -m depth; sensor at ~ 1 -m depth; sensor at ~ 1.5 -m depth, almost completely obscured. Calcium carbonate coccoliths are ubiquitous throughout the world ocean, and their optical effects are significant and easily measurable. Ocean acidification is expected to affect the abundance of calcium carbonate coccoliths, thereby causing fundamental changes in the optical properties of the sea.

ABSTRACT

The effects of ocean acidification (OA) are expected to be manifest over a broad range of spatial and temporal scales throughout the world ocean as the pH drops from the pre-industrial value of 8.2 to 7.8 by the year 2100. Calcifying plankton (like other biocalcifiers such as corals and shellfish) are expected to be strongly affected by OA because of their need for saturating carbonate conditions, which enables precipitation of calcium carbonate. Within the calcifying plankton, coccolithophores precipitate the smallest calcium carbonate particles (coccoliths), which are some of the strongest light-scattering particles in the sea. Thus, anything that will affect coccolithophore calcification (including OA) will likely affect the optical properties of the sea. Here, we describe the optical properties of coccolithophores and interpret some historical observations within the context of OA. Then, we discuss technologies that are available to measure optical properties of coccolithophores, and also how we could exploit coccolithophore optical properties to measure impacts of OA at different scales. We end with a discussion of the consequences (both optical and biogeochemical) of a “decalcified” surface ocean.

INTRODUCTION

As ocean pH drops from the pre-industrial value of 8.2 to 7.8 by the year 2100 (Feely et al., 2009), ocean acidification (OA) is predicted to have a complex combination of effects at all levels of the marine food web. Although major questions remain regarding microbial evolution and the rate at which communities can adapt to a more acidic ocean environment (Joint et al., 2009), there is good reason to believe that OA impacts could be significant. For example, within the microbial realm, any drop in seawater pH due to enhanced $p\text{CO}_2$ would change the proton gradient from outside to inside the cells, which would be expected to have impacts on numerous processes related to cell energetics, physiology, and growth. The same applies to phytoplankton and cyanobacteria, with photosynthesis being the obvious additional pH-sensitive process.

Within the division Haptophyta, coccolithophores fall within the class *Prymnesiophyceae* (scale-forming algae), which contains the order Coccolithales

(Edvardsen et al., 2000). These calcifying coccolithophores, ubiquitous throughout the euphotic regions of the global ocean, are unicellular algae that cover themselves with scales of calcium carbonate called coccoliths. The scales are several micrometers in diameter and either remain attached to the cells, surrounding them as interleaving “shields,” or they become detached into the water as solitary plates. Because coccolithophores rely on seawater being saturated for calcite, a decrease in pH due to OA would be expected to reduce calcification rates (Riebesell, 2004; see also opposing views of this conclusion in Iglesias-Rodriguez et al., 2008, and commentary by Riebesell et al., 2008).

OA effects could clearly be manifest further up the food web. Protozoan microzooplankton are voracious grazers in the sea, and some of them rely on the formation of calcium carbonate tests (e.g., foraminifera). Little is known about the impacts of OA on calcareous foraminifera (Bernhard et al., 2009a, 2009b), but, again, they rely on seawater

being supersaturated with the carbonate ion in order to precipitate CaCO_3 shells; in a lower-pH ocean, shell accretion likely would be more difficult (De Moel et al., 2009). This effect would be most pronounced in polar regions, where it is expected that they would be the first such waters to become undersaturated for calcite. Pteropods and other molluscan relatives also precipitate CaCO_3 (in the less-stable form aragonite), which here again is expected to be more thermodynamically difficult in an acidified ocean, especially in the polar regions (Fabry, 1989; Fabry and Deuser, 1991). Within the pelagic realm, there are calcifying meroplankton (larvae of urchins, sea stars, crustaceans, and mollusks) that might also be expected to be directly impacted by undersaturated waters associated with OA. Ultimately, OA effects on protozoa could cause second-order effects on phytoplankton due to “top-down” changes in grazing pressure.

COULD OCEAN ACIDIFICATION AFFECT THE SUBMARINE LIGHT FIELD?

To the extent that phytoplankton could be affected by OA, their associated optical properties also might change. Phytoplankton particulate organic carbon represents a significant source of light scattering within the sea, with a wavelength dependence of λ^{-1} (i.e., more scattering in the blue part of the spectrum than in the red; Stramski et al., 2007). Although water absorption is an important factor affecting photon propagation in the red and near-infrared part of the spectrum, phytoplankton absorption by photosynthetic pigments such as chlorophyll and associated accessory pigments has a major impact on the

attenuation of light in the blue (and red) parts of the spectrum (Yentsch, 1980). Along with algal chlorophyll, phytoplankton also produce photoprotective pigments to shield against damaging UV wavelengths; these pigments also modulate radiative transfer in the sea. Dissolved organic carbon (DOC) is excreted by phytoplankton, particularly when they are senescent or being grazed. A subset of that DOC, chromophoric dissolved organic matter (CDOM), has strong blue absorption, well into the UV end of the spectrum (Roesler and Perry, 1989). Given that phytoplankton can excrete as much as 30% of the fixed carbon as dissolved organic matter (Mague et al., 1980), their CDOM and detritus play a strong role in blue light absorption. However, recent evidence is equivocal on the effect of OA on DOC production. Engel et al. (2004) did not observe a statistically significant change in DOC production by the coccilithophore *E. huxleyi* under lower-pH conditions. On the other hand, using natural populations of phytoplankton from the Okhotsk Sea, Yoshimura et al. (2009) demonstrated a reduction in DOC production under more acidic conditions. Note that CDOM and particulate detritus are also exported from watersheds (including humic and fulvic materials produced by terrestrial vegetation; Benner, 1997), often dominating the optical properties of river-impacted

coastal waters (Babin et al., 2003). It is not known how OA would affect the overall chemistry, production, photo-oxidation, and microbial breakdown of optically active CDOM, whether derived from terrestrial or marine sources.

With such strong linkage between phytoplankton and the optical properties of in-water constituents, it logically follows that any effects of OA on the growth, grazing, and mortality of phytoplankton will also affect the ocean's bulk optical properties. This optical linkage could even control radiative transfer through the atmosphere. For example, it is well known that certain species of phytoplankton are strong producers of dimethylsulfide (Matrai and Keller, 1993; Wingenter et al., 2007). This gas, when released by phytoplankton, can diffuse across the air-sea interface and into the atmosphere, and act as cloud condensation nuclei, thus impacting cloud formation and sunlight propagation to the sea surface.

SUSPENDED CaCO_3 : A MAJOR MODULATOR OF THE SUBMARINE LIGHT FIELD

Particulate inorganic carbon (PIC, the generic name for CaCO_3) is a primary link between OA and ocean optical properties. Of all the particles found in the sea, PIC particles have a high index of refraction (1.19 relative to water), which means that PIC particles are much more efficient light scatterers than phytoplankton cells, or even biogenic silica (opal), both of which have relative refractive indices between 1.05 and 1.08 (Costello et al., 1995; Spinrad and Brown, 1986; Twardowski et al., 2001).

Given that OA is expected to have profound effects on calcifying plankton,

an obvious question is, how big would the optical impact be? To answer this question for calcium carbonate particles, we must first address whether all sizes and shapes of PIC particles are equal in terms of their light-scattering properties (note that PIC has negligible absorption [Balch et al., 1991]).

The effect of PIC particle size on light scattering can be modeled using anomalous diffraction theory (Van de Hulst, 1981), which implicitly assumes that particles are spherical. It also assumes that $n - 1 \ll 1$, (where n is the real part of the index of refraction), which is reasonable, but not strictly satisfied, for PIC. Based on this model, the most efficient PIC particles for light scattering (in terms of scattering per PIC concentration) are about 2 μm in diameter (Balch et al., 1996a). Above and below this diameter, the efficiency of light scattering falls off by orders of magnitude (Figure 1). The net result is that for ocean PIC particles, the light-scattering properties are most strongly dominated by coccolith-sized particles, not smaller ones (for which there are few examples, except broken coccoliths or aragonite needles, such as found in "whittings" [Broecker et al., 2000; Morse and He, 1993]) nor larger particles (such as foraminifera, pteropods, or invertebrate larvae tests). If there is any effect of OA on large PIC particles such as foraminifera or pteropods, it will make little difference to the bulk seawater optical properties, unless, of course, these large particles are orders of magnitude more abundant than normal, which seems unlikely. Typically, there are a few foraminifera animals per liter or several pteropods per cubic meter, whereas total coccolithophore

William M. Balch (bbalch@bigelow.org) is Senior Research Scientist, Bigelow Laboratory for Ocean Sciences, West Boothbay Harbor, ME, USA. Paul E. Utgoff (deceased) was Professor, Computer Science Department, University of Massachusetts, Amherst, MA, USA.

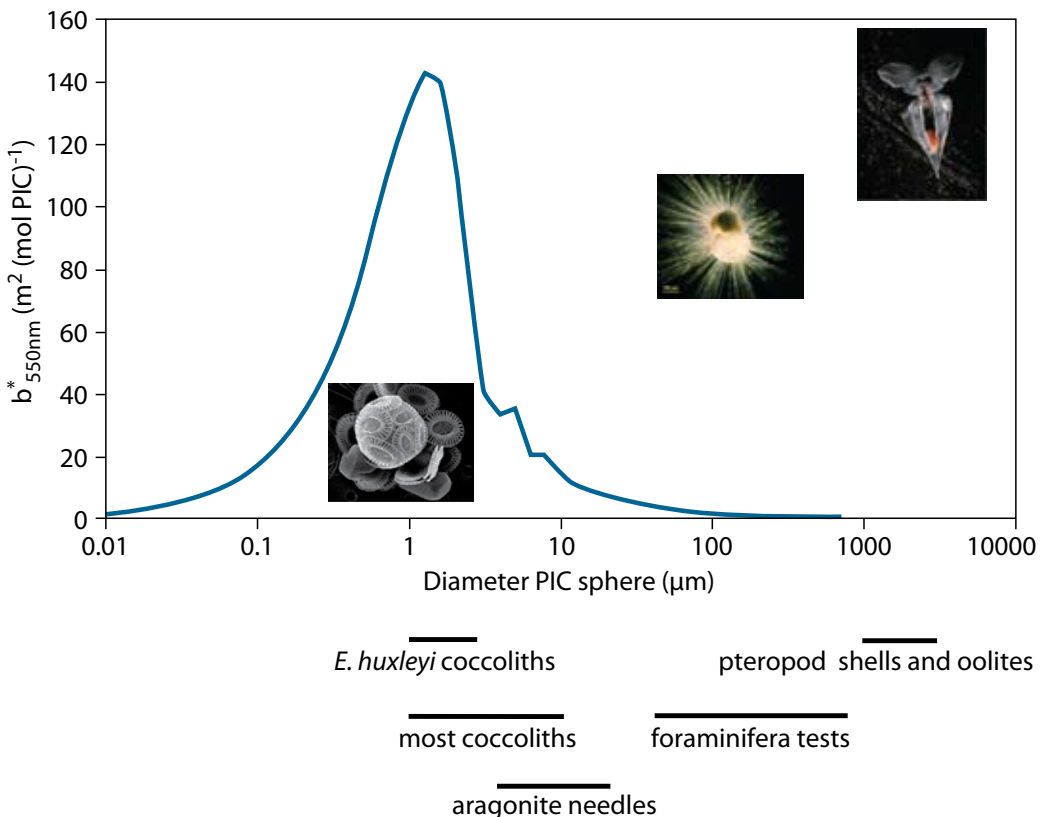


Figure 1. Theoretical calcite-specific scattering coefficient for calcite spheres vs. sphere diameter calculated with the anomalous diffraction theory (Van de Hulst, 1981). The size range extends from 0.01 to 10,000 μm . The approximate size ranges of some of the CaCO_3 particles found in the sea are shown for reference. This figure was modified from that originally published in Balch et al. (1996a) and extends the size range of PIC to larger particles. Insets, from left, show the coccolithophore *Emiliania huxleyi* (micrograph courtesy of J.M. Fortuño, Electron Microscopy Laboratory, Institute de Ciències del Mar, CSIC), the foraminifera *Globigerinella* sp. (image courtesy of O.R. Anderson; <http://starcentral.mbl.edu/microscope/portal.php?pagetitle=assetfactsheet&imageid=962&themeid=0>), and the pteropod *Clio pyramidata* (photo courtesy of Victoria Fabry, Cal State, San Marcos).

abundance in the most oligotrophic ocean waters is 10,000–100,000 L^{-1} (Haidar and Thierstein, 2001), and detached coccoliths will be 15–20 times that number. Thus, unlike foraminifera and pteropods, if OA affects coccolith or coccolithophore distributions, it should have strong impact on seawater optical properties.

Gordon and Du (2001) address the effect of coccolith shape on light scattering. They used the discrete dipole approximation (DDA) for *E. huxleyi* coccoliths to demonstrate that the total scattering cross section (and spectral variability) was similar for each of three particle shapes, in agreement with field *E. huxleyi* measurements. They observed strong dependence on particle morphology due to multiple reflections within the particles. Scattering and backscattering coefficients for volume-

equivalent spheres were within a factor of two of the DDA models. Given these observations, any change in PIC optical properties associated with OA would be more likely due to particle size than shape.

CaCO_3 , OCEAN HEATING, AND OCEAN ACIDIFICATION

A logical question to ask is, if OA affects coccolithophore abundance, would the heat budget of the surface ocean also be affected? Balch et al. (1996b, 2001) found that coccolithophorids account for 10–20% of total particle scattering of light in typical ocean waters, which increases to 90% in coccolithophorid blooms. Others have postulated that coccoliths might impact the ocean's heat budget (e.g., Ackleson et al., 1988). Tyrrell et al. (1999) modeled the radiative budget for water with and without

coccolithophores. They found that in water with a chlorophyll *a* concentration of 0.75 $\mu\text{g L}^{-1}$ and no coccolithophores (plus other physical factors as given in Figure 2), 6.9% of the incoming radiation would be scattered back out of the surface, 89.1% of the radiation would be absorbed over the top 20 m by water plus particulate matter, and 4.1% of the energy would propagate below the 20-m isobath (Figure 2A). Addition of PIC from a coccolithophore bloom ($300 \mu\text{gPIC L}^{-1}$) would increase ocean albedo to 11.4%, 87.8% of the energy would be absorbed in the top 20 m, and only 0.5% of the energy would propagate below the 20-m isobath (Figure 2B). The net effect was that the rate of change of temperature (in degrees Kelvin) due to adding $300 \mu\text{gPIC L}^{-1}$ would be $-5.66 \times 10^{-7} \text{ K s}^{-1}$ (Tyrrell et al., 1999) or about -0.033 K d^{-1} —significant cooling

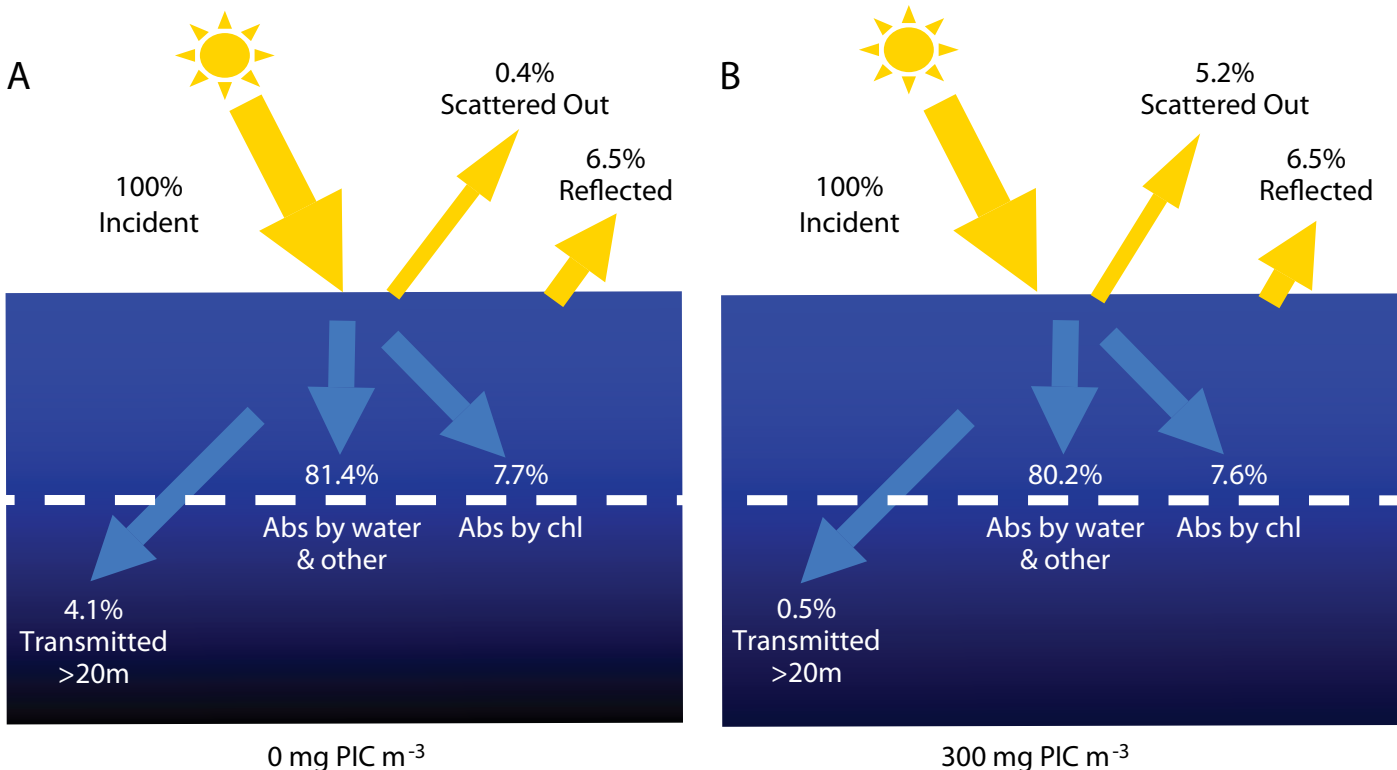


Figure 2. Photon budgets for water with (A) no particulate inorganic carbon (PIC) vs. (B) $300 \mu\text{g PIC L}^{-1}$. Values are based on incoming irradiance of $1100 \mu\text{Ein m}^{-2} \text{s}^{-1}$, wind speed = 5 m s^{-1} , cloud cover = 25%, chl = $0.75 \mu\text{g L}^{-1}$, and solar zenith angle = 45° . 1 Einstein = 1 mole of photons (or Avogadro's number of photons: 6.02×10^{23}). Optical modeling results redrawn from Tyrell et al. (1999)

when integrated over a typical bloom period of 30 d (-0.98 K). By inference, an acidified environment devoid of suspended coccolith calcite would be this much warmer. This effect on energy distribution will likely vary depending on the species of coccolithophores, due to significant differences in the calcite-specific backscattering cross sections of various coccoliths (Balch et al., 1999).

FOLLOWING OCEAN ACIDIFICATION THROUGH ITS EFFECTS ON PIC OPTICAL PROPERTIES

Ocean acidification is expected to have consequences throughout the global ocean, with a possible major impact on planktonic calcifiers. Because coccoliths can be a primary determinant of the submarine light field, it should be possible to invert ocean optical properties to quantitatively estimate PIC

concentration, which would be useful for examining OA. This link is particularly obvious when examining normalized water-leaving radiance (nL_w , defined as the upwelling radiance just above the sea surface, in the absence of an atmosphere, with the sun directly overhead) against PIC or coccolith concentration (Figure 3). Using nL_w data at 510 nanometers (nm) from the Gulf of Maine North Atlantic Time Series (GNATS), 20% of the variance in nL_w can be explained by PIC, and this increases to 38% when coccolith concentration is plotted against nL_w at 510, instead of PIC concentration. Indeed, our results show that this relationship is significant across the visible spectrum (albeit, correlations are best between 490–550 nm; data not shown). It is noteworthy to compare nL_w at 440 nm, the primary chlorophyll absorption wavelength, to the concentration of chlorophyll *a*, considered

to be the most important optically active component of the surface ocean. Such a plot for the GNATS data shows an *inverse* relationship that accounts for only 2% of the variance (data not shown). The inverse relationship is due to the fact that chlorophyll is absorbing light (thus reducing reflectance), whereas PIC intensely backscatters it (enhancing reflectance). Based on this statistically significant, first-order effect of PIC on nL_w , optical estimates of PIC might be the convenient way to document the impact of OA.

Optical methods for estimating PIC distributions fall into two categories: (1) *in situ* or bench-top measurements of inherent optical properties (IOPs, e.g., light scattering) and (2) passive remote sensing of visible and near infrared reflectance (i.e., measurement of apparent optical properties [AOPs], such as nL_w from ship or satellite). To assess

impacts of OA over basin scales, satellite remote sensing would be the optimal strategy. But, for smaller spatial and temporal scales, and for profiles of PIC over the water column, IOP measurements provide considerably more versatility. For example, consider the impact of the shoaling corrosive waters on the West Coast of North America (Feely et al., 2008), where such water may not yet have reached the surface layer visible to satellites. In this case, subsurface IOP measurements would be a preferable way to document the impact of OA on coccolithophores.

IOP MEASUREMENTS OF COCCOLITHOPHORE PIC

Two methods can be used to make IOP-based measurements of PIC. One method is to measure total backscattering and then to add a weak acid in order to drop the pH of the seawater/particle suspension below the dissociation point for calcite (which will dissolve calcite and the more-soluble aragonite), then remeasure backscattering. "Acid-labile backscattering" is calculated as the difference between total and acidified backscattering. This setup is ideal for semicontinuous shipboard measurements over a variety of spatial and temporal scales. Typically, acid-labile backscattering measurements can be made once every few minutes aboard ship, which allows spatial resolution of ~ 1 km at typical ship speeds. The technique is calibrated to particulate calcium measurements on filtered water samples made using inductively coupled plasma optical emission spectroscopy (ICPOES). An example of underway acid-labile backscattering measurements is shown for six different cruises across

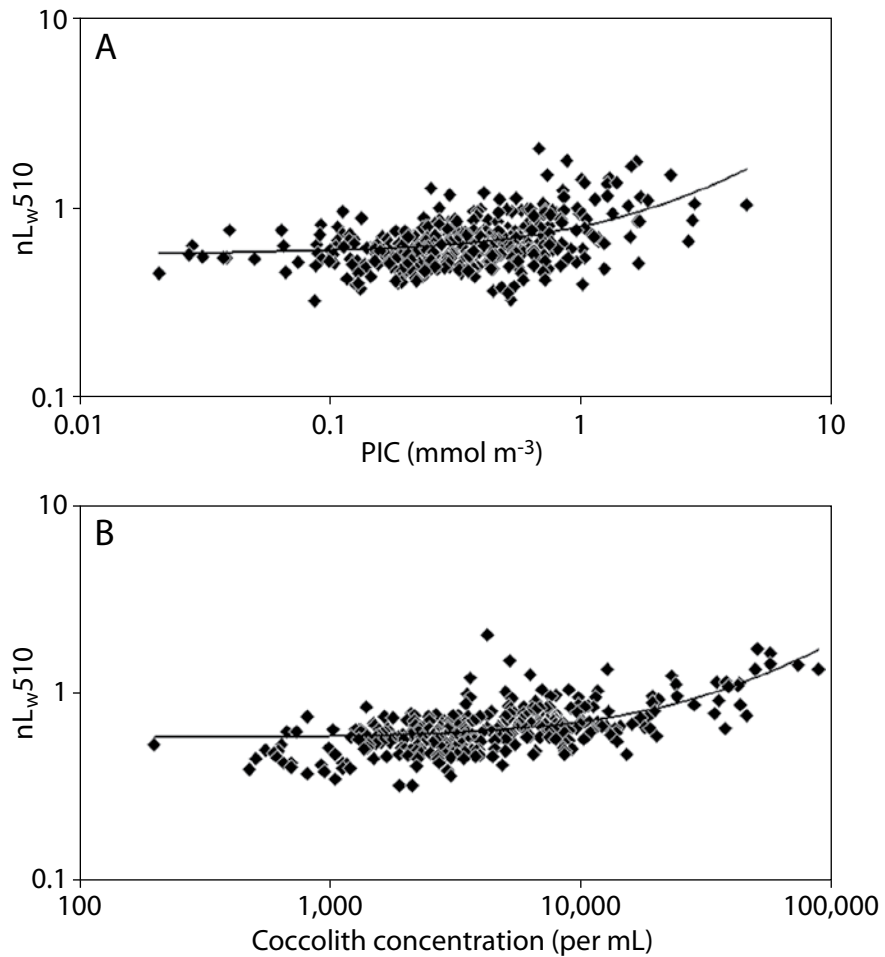


Figure 3. Above-water, normalized water-leaving radiance at 510 nanometers (nm) measured during 72 cruises across the Gulf of Maine for the Gulf of Maine North Atlantic Time Series (GNATS) between 1998 and 2006. Methodology for radiometry and particulate inorganic carbon (PIC) inductively coupled plasma optical emission spectroscopy measurements described elsewhere (Balch et al., 2008). Briefly, two Satlantic radiance sensors were mounted on the ship's bow, one pointed at 40° from nadir at the sea surface (to measure upwelling radiance), and one aimed at the sky, 40° from zenith (to measure downwelling sky radiance). The radiometers were kept at an azimuthal angle of 90–120° from the sun in order to minimize specular reflectance. A Satlantic irradiance sensor equipped with cosine collectors was aimed upward to measure downwelling sky radiance. Normalized water-leaving radiance was calculated from these measurements according to Mueller et al. (2003). (A) Water-leaving radiance at 510 nm plotted against PIC concentration. Least-squares fit to the data are: $Y[\pm 0.19] = 0.22[\pm 0.01]X + 0.57[\pm 0.01]$. Statistics for this fit are: $r^2 = 0.20$; DF = 447; P < 0.001 (where r^2 is the squared correlation coefficient, DF designates the degrees of freedom, and P is the probability that this relationship resulted purely by chance). (B) Water-leaving radiance at 510 nm plotted against the concentration of detached coccoliths. Least-squares fit to the data are: $Y[\pm 0.18] = 1 \times 10^{-5}[\pm 9.0 \times 10^{-7}]X + 0.58[\pm 0.01]$. Statistics for this fit are: $r^2 = 0.38$; DF = 323; P < 0.001. For both the least-squares fits, the values in square brackets represent the standard errors of the best-fit terms.

the Atlantic sector of the Antarctic Subpolar Front (Figure 4). The cruise results consistently show a region of elevated PIC across the Atlantic sector within the approximate vicinity of the Antarctic Subpolar Front. Conveniently (and fortuitously), due to the typical coccolith backscattering cross section, the magnitude of the acid-labile backscattering (in units m^{-1}) is approximately numerically equal to the PIC concentration (in moles m^{-3}). For OA studies, acid-labile backscattering measurements represent the maximum optical effect of a completely decalcified ocean (and we don't yet know the probability of such a scenario).

Another IOP method useful for studies of PIC and OA involves measuring PIC birefringence when the particles are illuminated with linearly

polarized light. This measurement can be made with a microscope or attenuation meter. Calcium carbonate has the optical property of rotating the plane of linearly polarized light by 90° . Thus, by illuminating particles with linearly polarized light and viewing them through a polarizing filter mounted orthogonally to the incident polarization plane, the particles appear bright against a dark background. Moreover, it appears that the amount of birefringence is a function of the amount of PIC (Beaufort, 2005).

Birefringence patterns of coccoliths are quite distinct, which aids in their identification (Moshkovitz and Osmond, 1989). This property has been invaluable for automated enumeration of coccoliths using microscopes (with image analysis that uses neural network software; Beaufort and Dollfus, 2004).

More recently, we designed and implemented an algorithm, "CCC" (Count Coccolithophores and Coccoliths), that takes advantage of the birefringence patterns for analysis of polarized microscope images for individual coccoliths as well as plated coccolithophores, both of which can be numerically important in the sea, contributing significant light scattering (Voss et al., 1998).

CCC analysis involves several important steps. It first quantifies (and eliminates) background light scattering in the image. Next, it estimates the birefringence of non-PIC particles in the image (which typically are more diffuse than PIC particles, with lower contrast). Next, CCC enumerates free coccoliths in the image (clusters of bright, birefringent pixels, arranged in distinctive patterns within a prescribed proximity

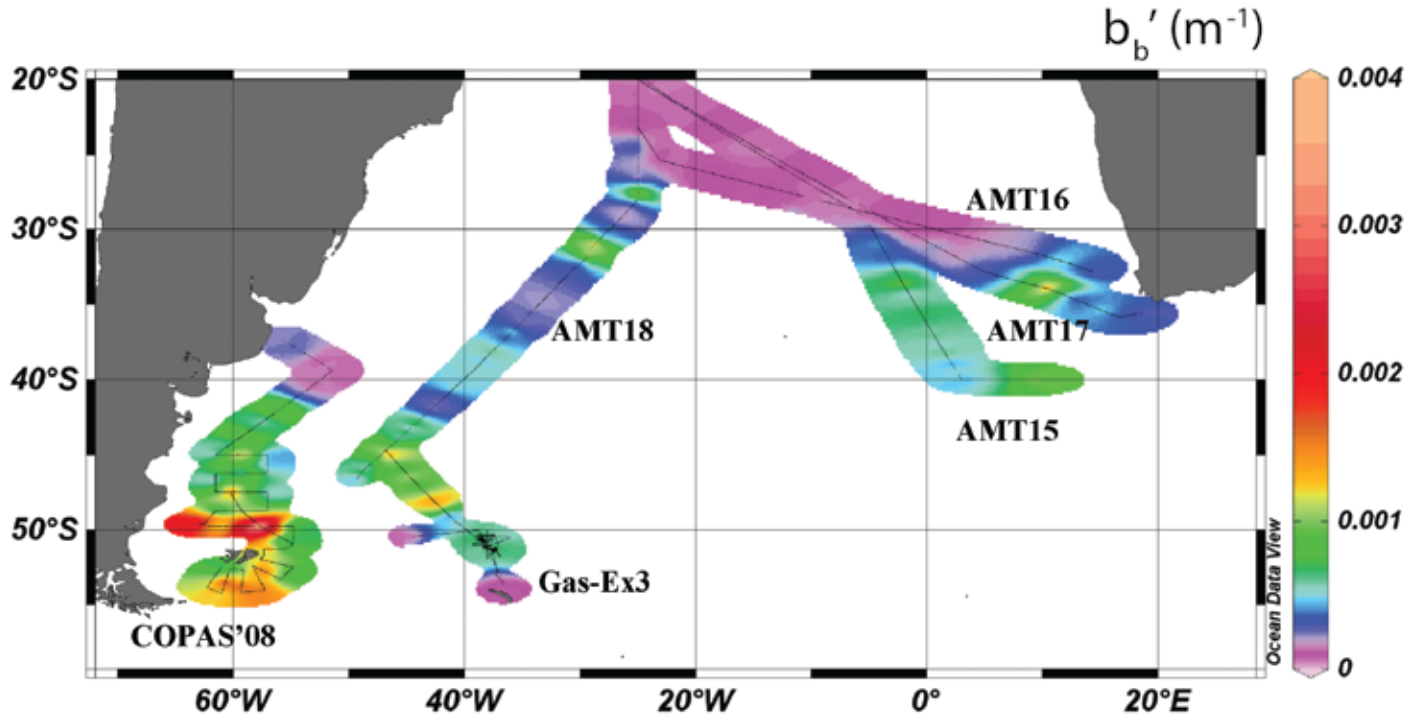


Figure 4. Acid-labile backscattering (b_b' ; units of m^{-1}) from six recent cruises to the South Atlantic: Atlantic Meridional Transect (AMT) 15 ('04), AMT 16 ('05), AMT 17 ('05), AMT 18 ('08), Gas-Ex3 ('07), and COPAS ('08). The first three cruises focused on the southeastern Atlantic while the latter three cruises focused in the southwestern Atlantic. Given the typical backscattering cross section of particulate inorganic carbon (PIC) coccoliths, there is roughly a 1:1 conversion between b_b' and PIC concentration (in units of moles m^{-3}).

of each other). Finally, it partitions the remaining birefringence patterns into (a) plated coccolithophores (having coccoliths, arranged in spherical patterns

with known diameters of plated coccolithophore cells and within a specific proximity of each other) or (b) randomly shaped coccolith aggregates (statistically

distinct from spherical coccolithophore cells) (Figure 5). Comparisons between CCC counts and manual microscope counts have been performed (results to

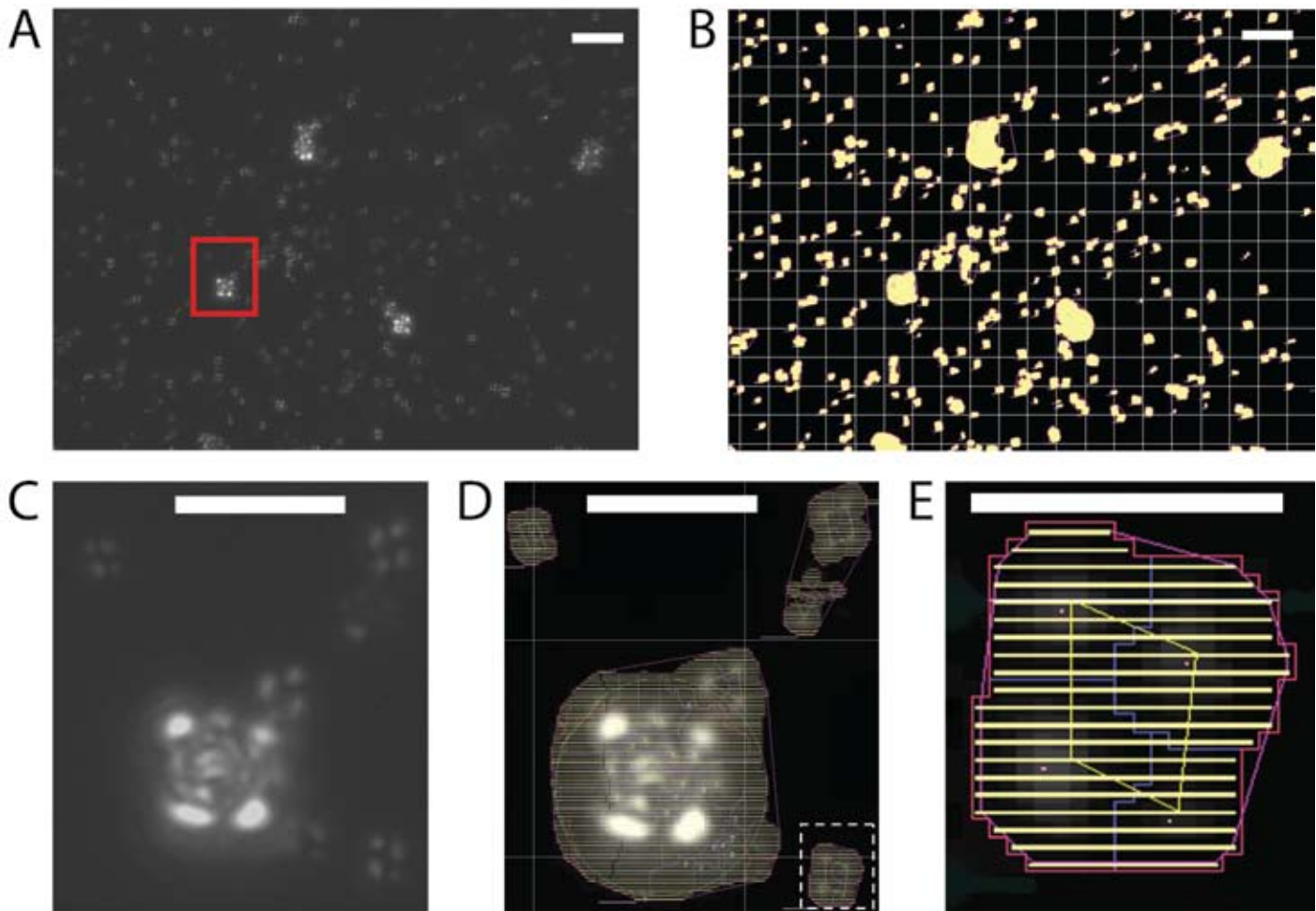


Figure 5. Count Coccolithophores and Coccoliths (CCC) algorithm analysis of birefringent microscope images of coccoliths and coccolithophores taken from a water sample of a bloom of the coccolithophore *Emiliania huxleyi* in the Gulf of Maine. The 50-mL seawater sample was filtered onto a 0.45- μm pore-size Millipore HA filter, then mounted in 60°C Canada Balsam on a glass microscope slide with a coverslip placed on top (Haidar and Thierstein, 2001). This treatment makes the filter transparent, after which the slide (with transparent filter) was viewed on a polarizing microscope. This microscope has two linear polarizers in the optical path, one above and one below the coccolithophore sample, with polarizers set orthogonally to each other; image is at 400X magnification. (A) Microscope birefringence image of coccoliths and plated coccolithophores. Detached coccoliths appear as four symmetrically oriented bright dots. Plated coccolithophores are seen as circular groups of white dots. Red square denotes subimage in panels C and D. White scale bar = 10 μm . (B) CCC-processed version of panel A. Pixels shaded in yellow are identified as either detached coccoliths or plated coccolithophores. White scale bar = 10 μm . (C) Blowup of subimage designated in panel A with one plated coccolithophore and several detached coccoliths. White scale bar = 5 μm . (D) CCC-processed subimage from panel C, better showing the discrimination of birefringent “peaks” in brightness, and their relative angular distribution (information also used in the discrimination of coccolith birefringent patterns). White dashed line denotes further subimage shown in panel E. White scale bar = 5 μm . (E) Blowup of subimage in panel D for a single coccolith. Thick, horizontal yellow lines represent horizontal rows of pixels. Red line denotes edge of coccolith with intensity significantly above slide background. Blue lines define illumination “lows” between each group of bright pixels. Pink dots denote highest irradiance value within each bright group of pixels. Yellow quadrangle defines relative orientation of “center of mass” of each bright group of pixels. The lavender line denotes the algorithm’s definition of particle, as distinct from other particles. This latter aspect is to discriminate solitary coccoliths from aggregates of coccoliths. White scale bar = 2 μm .

be published separately). CCC counts explain ~ ¾ of the variance in manual counts, and due to the high sensitivity of the microscope camera, CCC can discriminate distinct coccolith-specific birefringence patterns that are too dim to be discriminated by the human eye. Thus, CCC machine counts of coccoliths can be two to five times higher than human counts. Moreover, for dense coccolith-rich images, the images processed by CCC can be done about 400 times faster than manually processed images. A major rationale for the above software is that it will allow coccolith enumeration aboard autonomous platforms like drifting buoys or gliders, which will provide new insights into OA.

Guay and Bishop (2002) took advantage of CaCO_3 birefringence for in situ measurements of PIC using a beam transmissometer outfitted with orthogonal polarizers, one on either side of the seawater volume being viewed. The approach is ideal for in situ estimates of PIC whether from a suspended instrument or autonomous vehicle (Bishop, 2009). The method involves calibration of the instrument with pure suspensions of PIC particles. One potential limitation is that PIC is not the only birefringent material in the water (e.g., certain dinoflagellate thecae, zooplankton carapaces, and lipid-rich organelles are also birefringent; Balch and Fabry, 2008). Thus, optimal calibration should involve natural assemblages of particles with the particulate calcium concentration measured with ICPOES. This calibration then will account for any noncalcareous, birefringent particles in the assemblage (which could, admittedly, vary throughout the year and with depth, thus contributing to overall error). Like

the microscope techniques above, these in situ birefringence-based methods hold great promise for OA studies.

PASSIVE REMOTE-SENSING TECHNIQUES FOR COCCOLITHOPHORE PIC MEASUREMENTS

Satellite remote sensing offers the most promise for basin-scale studies of OA. Advances in remote-sensing technologies have been incremental. Turbid, high-scattering coccolithophore blooms were first described in Norwegian fjords (Berge, 1962). In the 1970s and 1980s, the Coastal Zone Color Scanner (CZCS) provided the first evidence of highly scattering mesoscale coccolithophore blooms. Blooms over the western European continental shelf were described with both CZCS (Holligan et al., 1983) and Landsat (Fevre et al., 1983). It was recognized that the intense scattering of coccoliths in otherwise clear ocean waters produced “anomalous Case I” conditions that could interfere with the radiance-based estimates of ocean chlorophyll from space (Gordon and Morel, 1983; Balch et al., 1989). Due to this strong optical effect, remote-sensing image “flags” were developed that would allow discrimination of coccolithophores present at high concentration (Brown and Yoder, 1993, 1994).

In the latter 1980s and 1990s, CZCS was no longer functional, so oceanographers used the broad, low-sensitivity visible-band channel of the Advanced Very High Resolution Radiometer (AVHRR) to locate coccolithophore blooms (Groom and Holligan, 1987). Turbid blooms were described using AVHRR in the Gulf of Maine (Balch et al., 1991) and the North Atlantic,

just south of Iceland (Holligan et al., 1993). The North Atlantic feature was the largest bloom of an algal species ever described, with an area of some half million square kilometers. During the 1990s, spectacular blooms appeared in the Bering Sea (Sukhanova and Flint, 1998; Stockwell et al., 2000; Napp and Hunt, 2001).

In 1997, NASA launched the ocean color satellite sensor SeaWiFS. Equipped with more spectral bands than CZCS, SeaWiFS had the potential to not only qualitatively describe coccolithophore blooms but also to quantify PIC concentrations. Using combined satellite/ship measurements, a three-band, turbid-water algorithm (Gordon et al., 2001) was developed that used SeaWiFS red and near-infrared radiance retrievals. This approach was a major advance, given that there was negligible interference from chlorophyll or CDOM (i.e., blue-absorbing substances) in the red and near-infrared bands. Moreover, the focus on red and near-infrared bands meant that atmospheric correction involved less extrapolation and was considerably more accurate. However, the three-band algorithm functions best to quantify PIC in turbid features but does not have the sensitivity to work in nonbloom waters where background, non-coccolithophore light scattering dominates (representative of most of the world ocean for most of the time).

To address quantitative PIC concentrations and OA studies in nonbloom waters, Balch et al. (2005) formulated a two-band PIC algorithm. This algorithm uses 440-nm and 550-nm bands and iteratively solves for both PIC and chlorophyll concentrations using absolute radiances (and their ratios) plus average

absorption and scattering properties of chlorophyll and coccoliths. The limitations of the two-band PIC algorithm are: (a) the use of absolute radiances for determination of in-water constituents involves more error than ratio algorithms (such as used for chlorophyll determination), (b) there is a larger atmospheric correction for blue-green radiances (i.e., greater extrapolation of the atmospheric correction from the near-infrared wavelengths to the blue-green wavelengths, which lowers accuracy), and (c) CDOM, with its high blue absorption, overlaps with chlorophyll absorption, which causes errors in PIC. The latter limitation means

that PIC determinations near river-dominated waters can be error prone. In order to estimate PIC most efficiently in both background and bloom waters, the three-band PIC algorithm has been merged with the two-band algorithm in the current NASA SeaDAS processing code. The global average PIC concentration for the entire Moderate Resolution Imaging Spectroradiometer (MODIS) Aqua mission (over seven years) shows the large-scale variability in coccolith PIC, with largest concentrations at high latitudes (considered the first regions that will become subsaturated for calcite saturation state due to OA; Feely et al., 2004; Figure 6).

PREDICTING OPTICAL CHANGES IN AN ACIDIFIED, "DECALCIFIED" OCEAN

Predicting OA-associated changes to the pelagic ocean environment will not be easy, given the complexities of interactions among ocean biology, chemistry, and physics. PIC particles, however, play such a pivotal role in a number of important processes that it is useful to focus our attention on the potential impact of OA on their loss (without replacement by other coccolithophore species). The discussion here is divided into potential direct radiative effects of OA and potential effects not related to optical properties (but that might be observable using

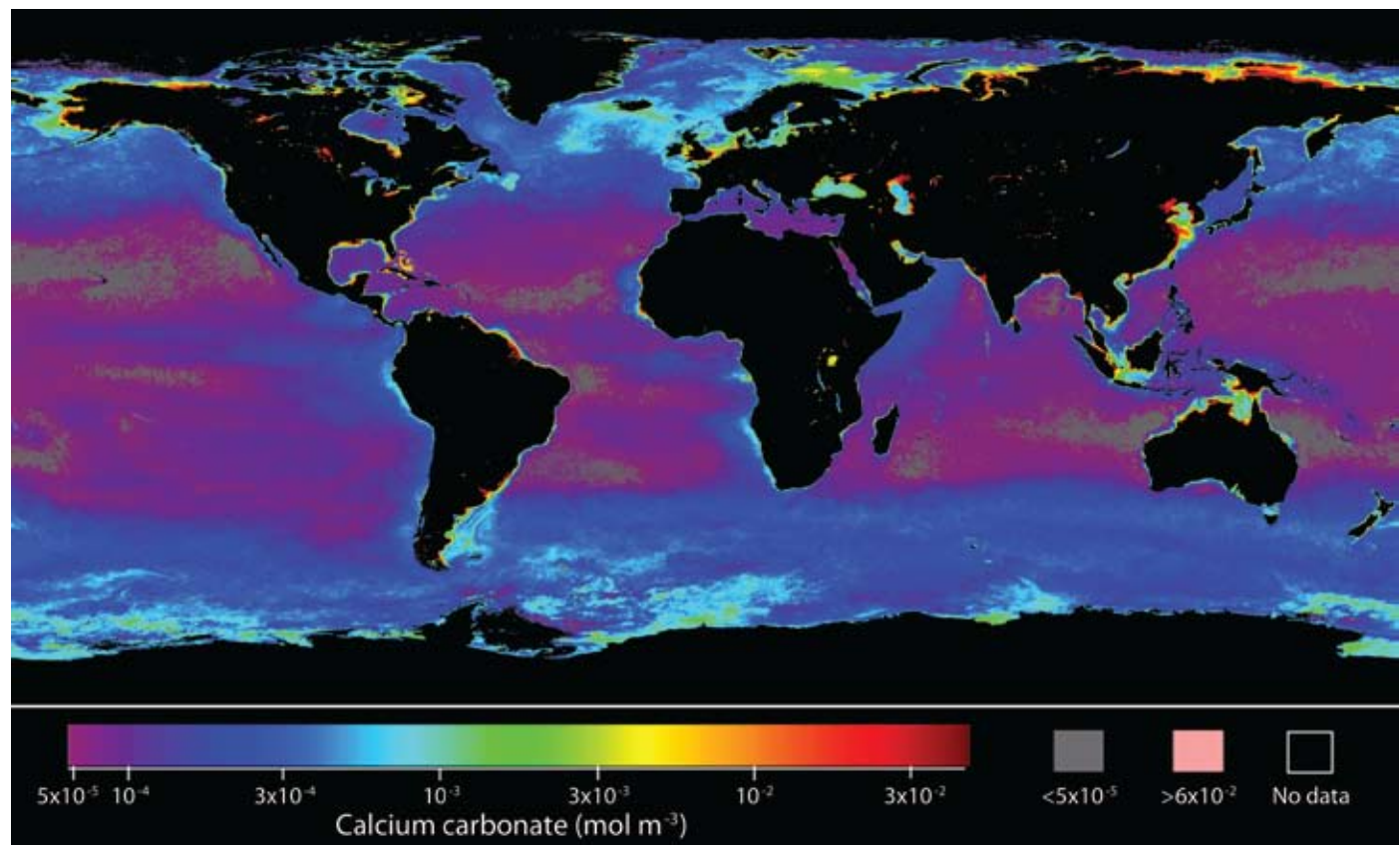


Figure 6. Merged two-band/three-band particulate inorganic carbon (PIC) algorithm showing coccolith PIC concentrations for the global ocean, averaged over the entire MODIS Aqua mission (January 1, 2002, to February 29, 2008). Color bar for PIC concentration (in mol PIC m⁻³) shown at lower left. Image produced by the NASA Ocean Color Group at the Goddard Space Flight Center

changes in optical properties).

The first, direct radiative effect of the loss of suspended PIC from the water column would be deepening of the euphotic zone. As noted above,

1994), then the K_d (550) would be 0.067 m^{-1} (for an attenuation length, or $1/K_d$, of $\sim 15 \text{ m}$). Further assuming that the euphotic zone extends to the 1% light level (4.6 attenuation lengths),

be considered in a “decalcified” ocean. That is, whether PIC particles have spectral scattering properties different from organic particles such that their removal might change the spectral qualities of the seawater suspension. Coccolith backscattering has been shown to have a spectral dependence of $\lambda^{-1.4}$ (Voss et al., 1998), not much different from organic particles (λ^{-1} for clearest ocean water; Morel, 1988). However, it has been realized since the first remote-sensing observations of coccolithophore blooms (Holligan et al., 1983) that the spectral qualities of the nL_w are markedly different from nonbloom waters, with the peak in nL_w shifting from the blue wavelengths to the blue-green wavelengths in blooms (Smyth et al., 2002). The net effect is that coccolithophore blooms are turquoise in color as shown in the graphic on the first page of this article. This spectral change is attributed to the considerably higher backscattering of PIC, relatively low absorption, and greater multiple scattering effects (Gordon et al., 2001; Smyth et al., 2002). Thus, for nonbloom waters (clearly, the majority of optical situations in the sea), it reasonably can be assumed that there would be a subtle spectral shift of the reflectance spectra toward blue wavelengths in the absence of coccolithophores. In short, OA could result in changes in both light quantity and spectral quality that could affect fundamental carbon fixation in the sea.

Such an increase in the euphotic depth would allow phytoplankton primary production to extend deeper in the water column, stripping nutrients deeper, which would presumably increase new production (Eppley and Peterson, 1979). Although these calculations are approximate, at best, they provide an order-of-magnitude estimate of the euphotic depth for a decalcified ocean.

Such an increase in the euphotic depth would allow phytoplankton primary production to extend deeper in the water column, stripping nutrients deeper, which would presumably increase new production (Eppley and Peterson, 1979). The other direct radiative effect of OA is that coccolithophore scattering could contribute to ocean cooling (Tyrrell et al., 1999) and, by inference, in waters devoid of coccolithophores, there would be more heating. In nonbloom waters, however, this heating effect presumably would be far more subtle than described for blooms.

Spectral effects of OA should also

typical acid-labile backscattering in non-coccolithophore bloom waters accounts for 10–20% of particle backscattering across the visible spectrum ($\sim 550 \text{ nm}$) (Balch et al., 2001). To relate this to euphotic zone depth, we must relate the IOPs to the AOPs, specifically the downwelling diffuse attenuation coefficient (K_d ; units of m^{-1}). A simple formulation for K_d (Gordon, 1989) is $K_d = 1.0395(a + b_b)/\bar{\mu}_d$, where a is the total absorption coefficient (m^{-1}), b_b is the total backscattering coefficient (m^{-1}), and $\bar{\mu}_d$ is the average cosine of the downwelling radiance field at a given depth (calculated as the downwelling irradiance divided by the downwelling scalar irradiance). As a simple example, data from the Atlantic Meridional Transect, which covers the central Atlantic from about 50°N to 50°S , commonly show mid-ocean absorption and backscattering values at 550 nm of about 0.04 m^{-1} and 0.01 m^{-1} , respectively (recent work of author Balch). Assuming typical $\bar{\mu}_d$ values of 0.75 for natural waters illuminated by sun and sky (Mobley,

is a strong correlation between CaCO_3 flux and both the magnitude (Klaas and Archer, 2002) and efficiency (Francois et al., 2002) of POC flux in deep (> 1000 m) sediment traps, which has led to the hypothesis of mineral ballast control of POC flux to depth (Armstrong et al., 2002). The mechanisms postulated to explain the correlation in deep traps are mineral protection of organic matter and/or the contribution of excess density of the sinking particles from the ballast minerals. The relative importance of coccolithophore vs. pteropod/foram calcification for the ballast mechanism is not yet clear. Indeed, the considerably larger foram and pteropod tests sink much more rapidly than individual coccoliths, but experiments have shown that aggregates with plated coccolithophores are tighter, with settling velocities significantly higher than noncalcifying coccolithophores (Engel et al., 2009). It is tempting to speculate that coccolithophore-dominated ecosystems (“carbonate ocean,” as coined by Honjo [1999]) may lead to tighter biologically mediated aggregates and more efficient export or, conversely, if OA inhibited coccolith formation, then less-efficient vertical transport of POC to deep waters (i.e., a slower biological pump) might be expected.

Along with slowing the biological pump, it might be reasonably assumed that the global rate of calcification would slow in an acidified ocean (Riebesell et al., 2000). This rate slowdown might be inferred from remote optical PIC measurements. Current estimates of pelagic calcification are about 0.8–1.6 Gt PIC yr^{-1} (Morse and Mackenzie, 1990; Archer and Maier-Reimer, 1994; Milliman et al., 1999;

Moore et al., 2002; Feely et al., 2004; Wollast, 1994; Balch et al., 2007), a large fraction of which sinks to the seafloor, where it dissolves or is buried. Calcification by coccolithophores produces an equimolar amount of CO_2 , which can enhance the $p\text{CO}_2$ of surface waters (Robertson et al., 1994; Bates et al., 1996), and it involves the removal of two times the number of moles of bicarbonate ions in surface waters. Thus, from a biogeochemical perspective, any reduction of calcification resulting from OA would slow the PIC burial (i.e., sequestration) term as well as the surface $p\text{CO}_2$ enhancement, and affect the alkalinity budget. In short, it is likely that the strong light scattering properties of coccolithophores, relative to other suspended particles in the sea, will provide the means to document OA-induced changes in biogeochemistry over entire ocean basins.

ACKNOWLEDGEMENTS

Bruce Bowler, Dave Drapeau, Emily Lyczkowski, Emily Booth, and Danielle Alley (Bigelow Laboratory for Ocean Sciences), Laura Windecker (University of California, Santa Barbara), and Elise Olson (Woods Hole Oceanographic Institution) helped with acquisition of field data presented in this paper. Allen R. Hanson, Howard J. Schultz, and Matthew B. Blaschko (University of Massachusetts Computer Science Department) helped with the original design of the CCC software and with interpretation of the model output following the untimely death of Paul E. Utgoff. Emmanuel Boss (University of Maine) and an anonymous reviewer provided helpful comments on an earlier draft of this manuscript. Support for this

work was generously provided by grants from NASA (grants NAS5-97268, NAS5-31363, NAG5-10622; NNG04GL11G; NNG04HZ25C, NNX07AD01G, NNX08AC27G), NSF (OCE-0136541; OCE-0325937; OCE 0728582), and ONR (N000140110042 and N00014-05-1-0111) to William M. Balch. Support for Paul E. Utgoff was generously provided by NSF (OCE-0325167). ☐

REFERENCES

- Ackleson, S., W.M. Balch, and P.M. Holligan. 1988. White waters of the Gulf of Maine. *Oceanography* 1(2):18–22. Available online at: http://tos.org/oceanography/issues/issue_archive/1_2.html (accessed November 11, 2009).
- Archer, D., and E. Maier-Reimer. 1994. Effect of deep-sea sedimentary calcite preservation on atmospheric CO_2 concentration. *Nature* 367:260–263.
- Armstrong, R.A., C. Lee, J.I. Hedges, S. Honjo, and S.G. Wakeham. 2002. A new, mechanistic model for organic carbon fluxes in the ocean based on the quantitative association of POC with ballast minerals. *Deep-Sea Research Part II* 49:219–236.
- Babin, M., D. Stramski, G.M. Ferrari, H. Claustre, A. Bricaud, G. Obolensky, and N. Hoepffner. 2003. Variations in the light absorption coefficients of phytoplankton, nonalgal particles, and dissolved organic matter in coastal waters around Europe. *Journal of Geophysical Research* 108(C7), 3211, doi:10.1029/2001JC000882.
- Balch, W.M., and V.J. Fabry. 2008. Ocean acidification: Documenting its impact on calcifying phytoplankton at basin scales. *Marine Ecology Progress Series* 373:239–247.
- Balch, W.M., D.T. Drapeau, B.C. Bowler, and E. Booth. 2007. Prediction of pelagic calcification rates using satellite-measurements. *Deep-Sea Research Part II (Chapman Calcification Conference Special Volume)* 54:478–495.
- Balch, W.M., D.T. Drapeau, B.C. Bowler, E.S. Booth, L.A. Windecker, and A. Ashe. 2008. Space-time variability of carbon standing stocks and fixation rates in the Gulf of Maine, along the GNATS transect between Portland, ME and Yarmouth, NS. *Journal of Plankton Research* 30:119–139.
- Balch, W.M., D.T. Drapeau, T.L. Cucci, R.D. Vaillancourt, K.A. Kilpatrick, and J.J. Fritz. 1999. Optical backscattering by calcifying algae—Separating the contribution by particulate inorganic and organic carbon fractions. *Journal of Geophysical Research* 104:1,541–1,558.

- Balch, W.M., D. Drapeau, J. Fritz, B. Bowler, and J. Nolan. 2001. Optical backscattering in the Arabian Sea: Continuous underway measurements of particulate inorganic and organic carbon. *Deep Sea Research Part I* 48:2,423–2,452.
- Balch, W.M., R.W. Eppley, M.R. Abbott, and F.M.H. Reid. 1989. Bias in satellite-derived pigment measurements due to coccolithophores and dinoflagellates. *Journal of Plankton Research* 11:575–581.
- Balch, W.M., H.R. Gordon, B.C. Bowler, D.T. Drapeau, and E.S. Booth. 2005. Calcium carbonate budgets in the surface global ocean based on MODIS data. *Journal of Geophysical Research* 110, C07001, doi:10.1029/2004JC002560.
- Balch, W.M., P.M. Holligan, S.G. Ackleson, and K.J. Voss. 1991. Biological and optical properties of mesoscale coccolithophore blooms in the Gulf of Maine. *Limnology and Oceanography* 36:629–643.
- Balch, W.M., K. Kilpatrick, P.M. Holligan, D. Harbour, and E. Fernandez. 1996a. The 1991 coccolithophore bloom in the central north Atlantic. II. Relating optics to coccolith concentration. *Limnology and Oceanography* 41:1,684–1,696.
- Balch, W.M., K.A. Kilpatrick, P.M. Holligan, and C. Trees. 1996b. The 1991 coccolithophore bloom in the central north Atlantic. I. Optical properties and factors affecting their distribution. *Limnology and Oceanography* 41:1,669–1,683.
- Bates, N.R., A.F. Michaels, and A.H. Knap. 1996. Alkalinity changes in the Sargasso Sea: Geochemical evidence of calcification? *Marine Chemistry* 51:347–358.
- Beaufort, L. 2005. Weight estimates of coccoliths using the optical properties (birefringence) of calcite. *Micropaleontology* 51:289–298.
- Beaufort, L., and D. Dollfus. 2004. Automatic recognition of coccoliths by dynamical neural networks. *Marine Micropaleontology* 51:57–73.
- Benner, R. 1997. Cycling of dissolved organic matter in the ocean. Pp. 317–332 (Chapter 12) in *Aquatic Humic Substances: Ecology and Biogeochemistry*. D. Hessen and L. Travik, eds., Springer-Verlag, New York.
- Berge, G. 1962. Discoloration of the sea due to *Coccolithus huxleyi* “bloom.” *Sarsia* 6:27–40.
- Bernhard, J.M., J.P. Barry, K.R. Buck, and V.R. Starczak. 2009a. Impact of intentionally injected carbon dioxide hydrate on deep-sea benthic foraminiferal survival. *Global Change Biology* 15:2,078–2,088.
- Bernhard, J.M., E. Mollo-Christensen, N. Eisenkolb, and V.R. Starczak. 2009b. Tolerance of allogromiid Foraminifera to severely elevated carbon dioxide concentrations: Implications to future ecosystem functioning and paleoceanographic interpretations. *Global and Planetary Change* 65:107–114.
- Bishop, J.K.B. 2009. Autonomous observations of the ocean biological carbon pump. *Oceanography* 22(2):182–193. Available online at: http://tos.org/oceanography/issues/issue_archive/22_2.html (accessed November 11, 2009).
- Broecker, W.S., A. Sanyal, and T. Takahashi. 2000. The origin of Bahamian whittings revisited. *Geophysical Research Letters* 27:3,759–3,760.
- Brown, C.W., and J.A. Yoder. 1993. Blooms of *Emiliania huxleyi* (Prymnesiophyceae) in surface waters of the Nova Scotian Shelf and the Grand Bank. *Journal of Plankton Research* 15:1,429–1,438.
- Brown, C.W., and J.A. Yoder. 1994. Coccolithophorid blooms in the global ocean. *Journal of Geophysical Research* 99:7,467–7,482.
- Costello, D.K., K.L. Carder, and W.L. Hou. 1995. Aggregation of diatom bloom in a mesocosm: Bulk and individual particle optical measurements. *Deep-Sea Research Part II* 42:29–45.
- De Moel, H., G.M. Ganssen, F.J.C. Peeters, S.J.A. Jung, G.J.A. Brummer, D. Kroon, and R.E. Zeebe. 2009. Planktic foraminiferal shell thinning in the Arabian Sea due to anthropogenic ocean acidification? *Biogeosciences Discussions* 6:1,811–1,835.
- Edvardsen, B., W. Eikrem, J.C. Green, R.A. Andersen, S.Y. Moon-Van der Staay, and L.K. Medlin. 2000. Phylogenetic reconstructions of the Haptophyta inferred from 18S ribosomal DNA sequences and available morphological data. *Phycologia* 39:19–35.
- Engel, A., L. Abramson, J. Szlosek, Z. Liu, G. Stewart, D. Hirschberg, and C. Lee. 2009. Investigating the effect of ballasting by CaCO₃ in *Emiliania huxleyi*. II. Decomposition of particulate organic matter. *Deep Sea Research Part II* 56:1,408–1,419.
- Engel, A., B. Delille, S. Jacquet, U. Riebesell, E. Rochelle-Newall, A. Terbruggen, and I. Zondervan. 2004. Transparent exopolymer particles and dissolved organic carbon production by *Emiliania huxleyi* exposed to different CO₂ concentrations: A mesocosm experiment. *Aquatic Microbial Ecology* 34:93–104.
- Eppley, R.W., and B. Peterson. 1979. Particulate organic matter flux and planktonic new production in the deep ocean. *Nature* 282:677–680.
- Fabry, V.J. 1989. Aragonite production by pteropod mollusks in the subarctic Pacific. *Deep-Sea Research Part I* 36:1,735–1,751.
- Fabry, V.J., and W.G. Deuser. 1991. Aragonite and magnesian calcite fluxes to the deep Sargasso Sea. *Deep-Sea Research* 38:713–728.
- Feeley, R.A., C. Sabine, J.M. Hernandez-Ayon, D. Ianson, and B. Hales. 2008. Evidence for upwelling of corrosive “acidified” water onto the continental shelf. *Science* 320:1,490–1,492.
- Feeley, R.A., C.L. Sabine, K. Lee, W. Berelson, J. Kleypas, V.J. Fabry, and F.J. Millero. 2004. Impact of anthropogenic CO₂ on the CaCO₃ system in the oceans. *Science* 305:362–366.
- Feeley, R.A., S.C. Doney, and S.R. Cooley. 2009. Ocean acidification: Present conditions and future changes in a high-CO₂ world. *Oceanography* 22(4):36–47.
- Fevre, J.L., M. Viollier, P.L. Corre, C. Dupouy, and J.R. Grall. 1983. Remote sensing observations of biological material by Landsat along a tidal thermal front and their relevancy to the available field data. *Estuarine, Coastal and Shelf Science* 16:37–50.
- Francois, R., S. Honjo, R. Krishfield, and S. Manganini. 2002. Factors controlling the flux of organic carbon to the bathypelagic zone of the ocean. *Global Biogeochemical Cycles* 16, doi:10.1029/2001GB001722.
- Gordon, H.R. 1989. Can the Lambert-Beer law be applied to the diffuse attenuation coefficient of ocean water? *Limnology and Oceanography* 34:1,389–1,409.
- Gordon, H.R., and T. Du. 2001. Light scattering by nonspherical particles: Application to coccoliths detached from *Emiliania huxleyi*. *Limnology and Oceanography* 46:1,438–1,454.
- Gordon, H.R., and A.Y. Morel. 1983. *Remote Assessment of Ocean Color for Interpretation of Satellite Visible Imagery: A Review*. Springer-Verlag, New York, 114 pp.
- Gordon, H.R., G.C. Boynton, W.M. Balch, S.B. Groom, D.S. Harbour, and T.J. Smyth. 2001. Retrieval of coccolithophore calcite concentration from SeaWiFS imagery. *Geochemical Research Letters* 28:1,587–1,590.
- Groom, S., and P.M. Holligan. 1987. Remote sensing of coccolithophore blooms. *Advances in Space Research* 7:73–78.
- Guay, C.K.H., and J.K.B. Bishop. 2002. A rapid birefringence method for measuring suspended CaCO₃ concentration in seawater. *Deep Sea Research Part I* 49:197–210.
- Haidar, A.T., and H.R. Thierstein. 2001. Coccolithophore dynamics off Bermuda (N. Atlantic). *Deep Sea Research* 48:1,925–1,956.
- Holligan, P.M., E. Fernandez, J. Aiken, W. Balch, P. Boyd, P. Burkhill, M. Finch, S. Groom, G. Malin, K. Muller, and others. 1993. A biogeochemical study of the coccolithophore, *Emiliania huxleyi*, in the north Atlantic. *Global Biogeochemical Cycles* 7:879–900.
- Holligan, P.M., M. Viollier, D.S. Harbour, P. Camus, and M. Champagne-Philippe. 1983. Satellite and ship studies of coccolithophore production along a continental shelf edge. *Nature* 304:339–342.
- Honjo, S., J. Dymond, W. Prell, and V. Ittekot. 1999. Monsoon-controlled export fluxes to the interior of the Arabian Sea. *Deep-Sea Research II* 46:1,859–1,902.
- Iglesias-Rodriguez, M.D., P.R. Halloran, R.E.M. Rickaby, I.R. Hall, E. Colmenero-Hidalgo, J.R. Gittins, D.R.H. Green, T. Tyrrell, S.J. Gibbs, P. von Dassow, and others. 2008. Phytoplankton calcification in a high-CO₂ world. *Science* 320:336–340.
- Joint, I., D.M. Karl, S.C. Doney, E.V. Armbrust, W.M. Balch, M. Beman, C. Bowler, M. Church, A. Dickson, J. Heidelberg, and others. 2009. *Consequences of High CO₂ and Ocean Acidification for Microbes in the Global Ocean*. Plymouth Marine Laboratory and Center for Microbial Oceanography: Research and Education (C-MORE), University of Hawaii, Honolulu, 23 pp.

- Klaas, C., and D.E. Archer. 2002. Association of sinking organic matter with various types of mineral ballast in the deep sea: Implications for the rain ratio. *Global Biogeochemical Cycles* 16, doi:10.1029/2001GB001765.
- Mague, T.H., E. Friberg, D.J. Hughes, and I. Morris. 1980. Extracellular release of carbon by marine phytoplankton: A physiological approach. *Limnology and Oceanography* 25:262–279.
- Matrai, P.A., and M.D. Keller. 1993. Dimethylsulfide in a large-scale coccolithophore bloom in the Gulf of Maine. *Continental Shelf Research* 13:831–843.
- Milliman, J., P.J. Troy, W. Balch, A.K. Adams, Y.-H. Li, and F.T. MacKenzie. 1999. Biologically-mediated dissolution of calcium carbonate above the chemical lysocline? *Deep-Sea Research Part I* 46:1,653–1,669.
- Mobley, C.D. 1994. *Light and Water: Radiative Transfer in Natural Waters*. Academic Press, New York, 592 pp.
- Moore, J.K., S.C. Doney, D.M. Glover, and I.Y. Fung. 2002. Iron cycling and nutrient-limitation patterns in surface waters of the world ocean. *Deep Sea Research Part II* 49:463–507.
- Morel, A. 1988. Optical modeling of the upper ocean in relation to its biogenous matter content (Case 1 waters). *Journal of Geophysical Research* 93:10,749–10,768.
- Morse, J.W., and S. He. 1993. Influences of T, S and $p\text{CO}_2$ on the pseudo-homogeneous precipitation of CaCO_3 from seawater: Implications for whiting formation. *Marine Chemistry* 41:291–297.
- Morse, J.W., and F.T. Mackenzie. 1990. *Geochemistry of Sedimentary Carbonates*. Elsevier Scientific Publishing Co., New York, 696 pp.
- Moshkovitz, S., and K. Osmond. 1989. The optical properties and microcrystallography of *Arkhangelskiellaceae* and some other calcareous nanofossils in the Late Cretaceous. Pp. 76–97 in *Nanofossils and Their Applications*. J.A. Crux and S.E. van Heck, eds, Ellis Horwood, Chichester.
- Mueller, J.L., A. Morel, R. Frouin, C. Davis, R. Arnone, K. Carder, Z.P. Lee, R.G. Steward, S.B. Hooker, C.D. Mobley, and others. 2003. Ocean Optics Protocols for Satellite Ocean Color Sensor Validation, rev. 4, vol. III: Radiometric Measurements and Data Analysis Protocols. Goddard Space Flight Center, Greenbelt, MD, 78 pp.
- Napp, J.M., and G.L.J. Hunt. 2001. Anomalous conditions in the south-eastern Bering Sea 1997: Linkages among climate, weather, ocean and biology. *Fisheries Oceanography* 10:61–68.
- Riebesell, U. 2004. Effects of CO_2 enrichment on marine phytoplankton. *Journal of Oceanography* 60:719–729.
- Riebesell, U., R.G.J. Bellerby, A. Engel, V.J. Fabry, D.A. Hutchins, T.B.H. Reusch, K.G. Schulz, and F.M.M. Morel. 2008. Comment on “Phytoplankton calcification in a high- CO_2 world.” *Science* 322(5907):1,466, doi:10.1126/science.1161096.
- Riebesell, U., I. Zondervan, B. Rost, P.D. Tortell, R.E. Zeebe, and F.M.M. Morel. 2000. Reduced calcification of marine plankton in response to increased atmospheric CO_2 . *Nature* 407:364–366.
- Robertson, J.E., C. Robinson, D.R. Turner, P. Holligan, A.J. Watson, P. Boyd, E. Fernandez, and M. Finch. 1994. The impact of a coccolithophore bloom on oceanic carbon uptake in the northeast Atlantic during summer 1991. *Deep Sea Research Part I* 41:297–314.
- Roesler, C.S., and M.J. Perry. 1989. Modeling in situ phytoplankton absorption from total absorption spectra in productive inland marine waters. *Limnology and Oceanography* 34:1,510–1,523.
- Smyth, T.J., G.F. Moore, S.B. Groom, P.E. Land, and T. Tyrrell. 2002. Optical modeling and measurements of a coccolithophore bloom. *Applied Optics* 41:7,679–7,688.
- Spinrad, R.W., and J.F. Brown. 1986. Relative real refractive index of marine microorganisms: A technique for flow cytometric estimation. *Applied Optics* 25:1,930–1,934.
- Stockwell, D.A., T.E. Whittle, T. Rho, P.J. Stabeno, K.O. Coyle, J.M. Napp, S.I. Zeeman, and G.L. Hunt. 2000. Field observations in the Southeastern Bering Sea during three years with extensive coccolithophorid blooms. Paper presented at AGU/ASLO Ocean Sciences Meeting, January 24–28, 2000, San Antonio, Texas. *Eos, Transactions, American Geophysical Union* 80: OS41.
- Stramski, D., R.A. Reynolds, M. Babin, S. Kaczmarek, M.R. Lewis, R. Rottgers, A. Sciandra, M. Stramska, M. Twardowski, and H. Claustre. 2007. Relationships between the surface concentration of particulate organic carbon and optical properties in the eastern South Pacific and eastern Atlantic oceans. *Biogeosciences Discussions* 4:3,453–3,530.
- Sukhanova, I.N., and M.V. Flint. 1998. Anomalous blooming of coccolithophorids over the eastern Bering Sea shelf. *Oceanology* 38:502–505.
- Twardowski, M.S., E. Boss, J.B. Macdonald, W.S. Pegau, A.H. Barnard, and J.R.V. Zaneveld. 2001. A model for estimating bulk refractive index from the optical backscattering ratio and the implications for understanding particle composition in case I and case II waters. *Journal of Geophysical Research* 106:129–14.
- Tyrrell, T., P.M. Holligan, and C.D. Mobley. 1999. Optical impacts of oceanic coccolithophore blooms. *Journal of Geophysical Research* 104:3,223–3,241.
- Van de Hulst, H.C. 1981. *Light Scattering By Small Particles*. Dover publications, Mineola, NY, 470 pp.
- Voss, K., W.M. Balch, and K.A. Kilpatrick. 1998. Scattering and attenuation properties of *Emiliania huxleyi* cells and their detached coccoliths. *Limnology and Oceanography* 43:870–876.
- Wingenter, O.W., K.B. Haase, M. Zeigler, D.R. Blake, F.S. Rowland, B.C. Sive, A. Paulino, R. Thyrhaug, A. Larsen, K. Schulz, and others. 2007. Unexpected consequences of increasing CO_2 and ocean acidity on marine production of DMS and CH₂ClI: Potential climate impacts. *Geophysical Research Letters* 34, L05710, doi:10.1029/2006GL028139.
- Wollast, R. 1994. The relative importance of biominerization and dissolution of CaCO_3 in the global carbon cycle. Pp. 13–35 in *Bulletin de l’Institut Oceanographique*, Special Vol. No. 13. F. Doumenge, D. Allemand, and A. Toulemon, eds, Musée Oceanographique, Monaco.
- Yentsch, C.S. 1980. Light attenuation and phytoplankton photosynthesis. Pp. 95–127 in *The Physiological Ecology of Phytoplankton*. I. Morris, ed., University of California Press, Berkeley, CA.
- Yoshimura, T., J. Nishioka, K. Suzuki, H. Hattori, H. Kirosawa, and Y.W. Watanabe. 2009. Impacts of elevated CO_2 on phytoplankton community composition and organic carbon dynamics in nutrient-depleted Okhotsk Sea surface waters. *Biogeosciences Discussions* 6:4,143–4,163.